Numerical Studies on Propellers in Open Water and behind Hulls aiming to support the Evaluation of Propulsion Tests

Article · October 2016

8 authors, including:

Heinrich Streckwall
Hamburgische Schiffbau-Versuchsanstalt Gm…
19 PUBLICATIONS   59 CITATIONS

SEE PROFILE

Tomasz Bugalski
Ship Design and Research Centre (CTO S.A.)
13 PUBLICATIONS   13 CITATIONS

SEE PROFILE

Lars Greitsch
Mecklenburger Metallguss GmbH
8 PUBLICATIONS   7 CITATIONS

SEE PROFILE

Numerical Studies on Propellers in Open Water and behind Hulls aiming to support the Evaluation of Propulsion Tests

Heinrich Streckwall[*] and Thomas Lücke[*], Tomasz Bugalski[†] and Judyta Felicjancik[††],
Tom Goedicke[‡] and Lars Greitsch[‡], Alaz Talay[§] and Mustafa Alvar[§]
[*]HSVA, Hamburg/Germany, [†]CTO, Gdansk, Poland, [††]Gdańsk Univ. of Technology, Poland
[‡]MMG, Waren, Germany, [§]MILPER Istanbul, Turkey   streckwall@hsva.com

1 Introduction

A RANS based numerical analysis of propellers can contribute considerably to our understanding of propeller/hull interaction. It may also allow for a review of scaling procedures on results from experimental fluid dynamics (EFD). Using various RANS codes (Fluent, CFX, STAR-CCM+ and FreSCo+) on common test cases the authors first focused on propeller open water (POW) calculations. Next we simulated the propeller hull interaction for two in-behind cases and processed results in close comparison with the POW analysis.

2 Content

One of the treated propellers – CPP 1304 - was released as a public test case several years ago and in 2016 also served for scale effect studies in an ITTC-Benchmark call. For the CPP 1304 our viscous calculations include POW setups (treating model/full scale and hub cap variants). Also an inclined flow and an in-behind case - with a body of revolution (BoR) ahead - are treated. The other propeller - CP 469 - is working behind the research vessel 'Nawigator'. CP 469 is also analyzed in POW mode and 'in-behind' with the 'Nawigator' hull ahead. For propellers working in-behind, the dual mesh methodology - a fixed mesh covering the hull and outer boundaries / a moving mesh capturing the propeller – represents the genuine approach within a RANS based analysis. For the POW mode a single rotating mesh including also the outer borders would be sufficient. Here, to allow for a thorough comparison of forces and moments when switching from in-behind to POW, the dual mesh methodology was also applied to simulate the POW setup. Moreover, for consistency, the moving mesh part containing the propeller blades was taken over 1:1 to serve also as sub-mesh for the propulsion mode.

3 Results for a propeller in open water and under inclined flow

It is considered that 3 effects cause deviations between POW results from EFD and CFD: a) boundary layer development, b) hub cap force with blades mounted and absent and c) resolution of the vortex wake structures.

3.1 Comparing with model tests

In the usual POW mode the hub cap is pointing upstream. A RANS analysis done under such conditions for the CPP 1304 shows a considerable reduction of the nominal cap resistance ('nominal'=cap subject to free stream / blades absent). With blades present a low-pressure field at their roots extends upstream and influences the hub cap forces. This effect may compensate the stagnation pressure contribution (see Fig. 1). If the comparison of axial forces from POW tests and POW calculations is re-considered by introducing calculated hub cap forces, the thrust curves (KT) come closer together as shown in Fig. 2. Fig. 2 also contains a comparison of HSVA's 'FreSCo+' results using the two different mesh methodologies for the rotating propeller.
The inclined flow case represents a first step into the direction of propeller/wake interaction. For the CPP 1304 related tests under an inclination of 12° were available. Fig. 3 gives the comparison of test results and 'FreSCo+'-calculations. Here the advance coefficient J involves the velocity magnitude of the incoming flow.

3.2 Changing Scales for the propeller CPP 1304

For the CPP 1304 the ITTC-Benchmark call was requesting a numerical scaling of POW data. Table 1 below gives the dimensions, rates and surface conditions which we applied to the two scales of propeller 1304. It has to be noted that the original request for the ITTC-Benchmark call was a roughness setting of 10 microns ($10*10^{-06}$ m) in full scale. In this paper an 'extreme' case is considered in addition, namely a 'slip wall' setting for the blades. Fig. 4 displays the POW performances calculated under the three above mentioned conditions.
An interesting effect was registered when we plotted the surface pressure. In Fig. 5 Model Scale pressure results and in-viscid pressure are displayed section wise. The trailing edge pressure at inner sections may show a pronounced sensitivity to the 'slip wall' setting. This effect is reduced if one moves into the direction of the tip.

			(FS)	(Mo)
Diameter	DP	[m]	3	0.25
blade roughness	kp	[m]	0.00E+00	0.00E+00
rate of revolution	n	[s-1]	4.33	15

Table 1: Dimensions, rates and surface conditions for the Model Scale and Full Scale versions of CPP 1304

4 In-behind results

The above mentioned consistent treatment of the POW setup and the propulsion mode was applied for 2 cases. The 'Nawigator', a standard single screw ship, represents Case 1 and an artificial fully wetted body with rotational symmetric shape defines Case 2. This artificial body of revolution (BoR) was driven by the CPP 1304.

4.1 Body of revolution (BoR)

Using HSVA's 'FreSCo+' for the BoR, pure resistance calculations served to confirm, that a reasonable axial wake field develops at the propeller plane. It was also intended to separate the axial wake into a contribution caused by displacement (potential flow) and an influence from viscous effects. The relevant wakes are given in Fig. 6. The distribution labeled 'viscous' in Fig. 6 is considered a typical circumferential mean axial velocity profile measured behind a single screw hull. For the mounted propeller we used the sliding interface technique to simulate rotation. The bare propeller blade forces at CPP 1304 and the reaction of the body were monitored (Fig. 7). A considerable suction force was acting on the downstream hub cap (Fig. 8).

Further studies were addressing thrust deduction. We evaluated the force difference between the pure resistance mode and the propulsion mode. This was done for the viscous flow case and the artificial in-viscid treatment of the body. The propeller (simulated 'viscous' in any case here) was kept at 15 Hz and the inflow velocity was set to 5 m/s. Combining these two settings formally to a J-value (D=0.25 m) gives formally J=1.33. The latter setting would cause a lightly loaded propeller for POW conditions. The wake effect raises thrust and torque. Note that we have no self-propulsion situation here. In the viscous case the forces on the body relate to roughly 60% of propeller thrust T. When the body is treated in-viscid they amount to roughly 13% of T. However evaluating thrust deduction values T-R_T, we arrive at very similar thrust deduction to thrust ratios (Fig. 9).

4.2 'Nawigator' by HSVA using HSVA's 'FreSCo+' code

The 'Nawigator'- propulsion was modeled via the double body approach with prescribed RPM. A process similar to the standard propulsion test (PT) evaluation was invoked.

The influence of the rudder's presence onto the propulsion behavior is studied especially from the propeller point of view. Even if this topic is not comparable with available model test results, it is worth to take a look into its influence. Slices on mid ship through each calculation domain are given in Fig. 10. The evaluation of the propulsion prediction is here based on a POW characteristic, performed in reverse mode, which means, with an upstream-located shaft (with slip wall condition) and with the original propeller cap pointing downstream (see Fig. 10 below). Using this constellation the evaluation is made in the most consistent manner. The above mentioned discussion about the hub's influence onto the POW results can be avoided. Of course the comparability with test results is weakened.

It turned out, that as a kind of reverse engineering, the target y+ setting on the propeller blades needed to be varied until the POW characteristic as well as the propulsion characteristic were represented reasonable. This approach is understood as an engineering work-around for this kind of design predictions to balance (besides other possible errors) the gap between the fully turbulent flow assumption in the applied RANS solution and the real flow around the blades, which can contain a high amount of laminar flow.

The y+ target of about 120 led to acceptable results for the POW condition, whereas the target y+ of about 70 was to be chosen for the propeller behind the ship model, see Table 2 for the comparison with the experiments.

	KT0	10KQ0	etaD	eta0	etaR	etaB	etaH	weff	N (Hz)	THDF
CTO EFD	0.249	0.365	0.622	0.482	**1.002**	**0.484**	1.287	0.418	10.36	0.2510
HSVA CFD	0.245	0.363	0.620	0.476	**1.015**	**0.484**	1.283	0.416	10.44	0.2510
difference (%)	**-1.6%**	**-0.5%**	**-0.3%**	**-1.2%**	**1.3%**	**0.0%**	**-0.3%**	**-0.5%**	**0.7%**	**0.0%**

Table 2: EFD-CFD comparison, Vs=11kts

The predicted η_R =1.015 is 1.3% higher than η_R from experiment. From the propeller and from the consistency point of view, the important result is the coincidence of the in behind efficiency $\eta_B = \eta_0 * \eta_R = T*Vs*(1-weff)/PD$, which relates the increase of η_R to the decrease of η_0 and to a still inappropriate POW representation. After finding the appropriate y+ setting the influence of different boundary conditions onto the propulsion results, especially on η_R, could finally be investigated, as there are: (a) the influence of the presence of the rudder and (b) a slip-wall boundary condition on the propeller.

The first approach (a) can be investigated by experiments as well, whereas the second (b) is only possible to be achieved numerically. This academic boundary condition has the practical advantage of being relative insensible to issues like Reynolds-Number and related uncertainty of the applied grid resolution (see above). It is assumed that the results (KT and KQ) will be free of scale effects.

	KT0	10KQ0	etaD	eta0	**etaR**	etaB	etaH	N (Hz)	weff	**THDF**
w/o rudder	0.232	0.348	0.601	0.5	**0.997**	0.498	1.207	10.548	0.372	0.2419
with rudder	0.245	0.363	0.620	0.476	**1.015**	0.484	1.283	10.435	0.416	0.2510
difference (%)	**5.6%**	**4.3%**	**3.2%**	**-4.8%**	**1.8%**	**-2.8%**	**6.3%**	**-1.1%**	**11.8%**	**3.8%**

Table 3: Influence of rudder, Vs=11kts

The main influence of the rudder onto the propulsion behavior turned out to be an increased hull efficiency η_H by 6.3% and a reduced η_B by 2.8%, see Table 3. From the propeller point of view this leads via a reduction of η_0 by 4.8% to higher η_R of 1.8%. As expected, the longitudinal force acting on the propeller cap turned out to be a resistance at POW-condition (-0.8% of KT) as well as for the case w/o rudder (-0.07% of KT), but due to the presence of the rudder the force became a thrust! +1.2% of KT. A slice on mid ship through each calculation domain is given in Fig. 10 for both in behind cases as well as for the open water case, showing the total velocity fraction V/U0. The main difference due to the rudder is found to be the diffusion of the propeller slip stream radius and especially the less concentrated vortex core compared to the case w/o rudder and the POW condition. Independent of the applied wall boundary condition on the propeller (non-slip-wall/slip-wall) the influence of the rudder onto η_R is predicted to be very similar (higher η_R of 1.7%), see Table 4. So the viscous effects seem to be limited in this respect and it becomes a pressure related benefit w/o increased torque.

slip-wall	KT0	10KQ0	etaD	eta0	**etaR**	etaB	etaH	N (Hz)	weff	THDF
w/o rudder	0.237	0.323	0.690	0.555	**1.019**	0.565	1.220	10.36	0.379	0.2419
with rudder	0.253	0.341	0.702	0.521	**1.036**	0.540	1.298	10.36	0.423	0.2510
difference (%)	**6.8%**	**5.6%**	**1.7%**	**-6.1%**	**1.7%**	**-4.4%**	**6.4%**	**0.0%**	**11.6%**	**3.8%**

Table 4: Influence of rudder, Vs=11kts, slip-wall condition on propeller blades only, same N

Naturally the missing shear stress on the propeller at slip-wall condition increases KT and reduces KQ as expected, see Fig. 11. Since the propulsion case as well as the POW case is treated in the same manner, the propulsion evaluation should show more or less the same η_R, which is obviously not the case (slip-wall 1.036 Tab. 4 vs. non-slip-wall 1.015, Tab. 3). The reason can be related to a numerical inaccuracy which alters the flow characteristic at POW condition differently than at the PT condition. Besides this, it possibly shows the remaining unresolved scale effect and serves as an outlook onto η_R beyond full scale RN.

4.3 'Nawigator' by MMG

Fig. 12 shows the development of η_R comparing in behind torque with open water torque calculated at different RN. The experimental result could be reproduced with very good accuracy. When decreasing the open water RN towards the level of the in behind situation there is a clear increase in η_R. A viscous scale effect on η_R as well as a reliably recommendation of a CFD supported propulsion analysis is targeted with the results of full scale calculations at same RN in open water and in behind conditions.

4.4 'Nawigator' by MILPER using ANSYS 'Fluent'

Calculations are done viscid and in-viscid for η_R estimation. The POW analysis was set up in reverse mode. POW characteristics are shared in Fig. 13. The procedure for the open water calculations is similar to the HSVA's approach (previously mentioned). There were two main focus points for the investigation of the propeller performance including the hull, namely the validation of the propulsion point and the rudder effect. The propulsion point is determined in two operating conditions using the double body approach (see Table 5). η_R is calculated using an interpolation function on the open water efficiency calculations done beforehand. The

effect of the rudder is related to an extra high pressure field, increasing the propeller thrust while increasing the torque as well. According to the CFD analysis, if the quality of performance is expressed by η_R, the propeller performs better with the rudder since thrust increases more than torque.

	Vm (m/s)	n (rps)	T - CFD (N)	T - Test (N)	ERROR	Q - CFD (Nm)	Q - Test (Nm)	ERROR
with rudder	1.301	6.91	28.97	29.67	2.37%	0.993	0.997	0.41%
	1.789	10.36	68.89	69.58	1.00%	2.300	2.301	0.05%
w/o rudder	1.301	6.91	26.814			0.957		

Table 5: Propeller performance in behind the Nawigator hull, Influence of rudder, Vs=11kts

5 Conclusion and Acknowledgement

In an on-going project we studied the performance of propellers in various flow environments. A combined treatment of the POW and in-behind setup allows judging the power saving quality of a wake adapted propeller. The power at POW under thrust- and RPS-identity is the reference. This is linked to the processing of performance data obtained via model tests, where the 'relative rotative efficiency' η_R is derived as quality index for wake adaption. The problem and challenge of the test evaluation process lies in the removal of any Reynolds-number dependence from η_R (POW tests are usually done at higher Reynolds-numbers than the related propulsion tests). Here CFD may support the test evaluation.
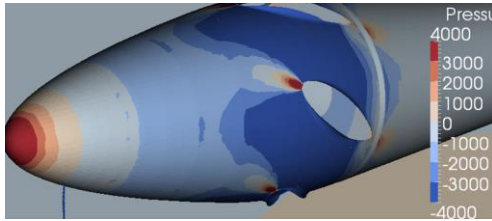
Fig. 1: Upstream cap of CPP 1304 in POW mode

Fig. 3: CPP 1304 inclined flow results (12°)

Fig. 2: CPP 1304 open water results
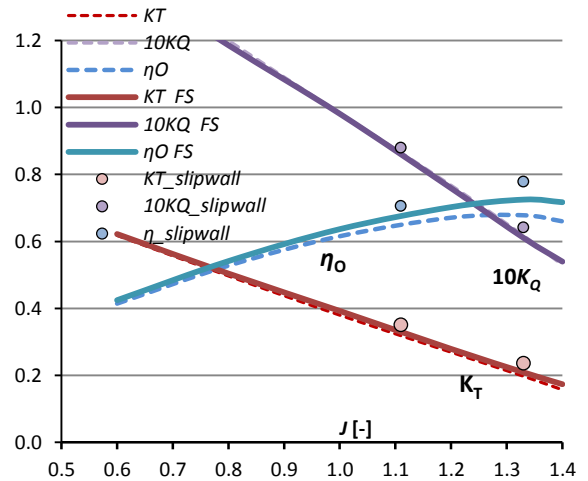
Fig. 4: POW RANS results (two scales and 'slip wall')
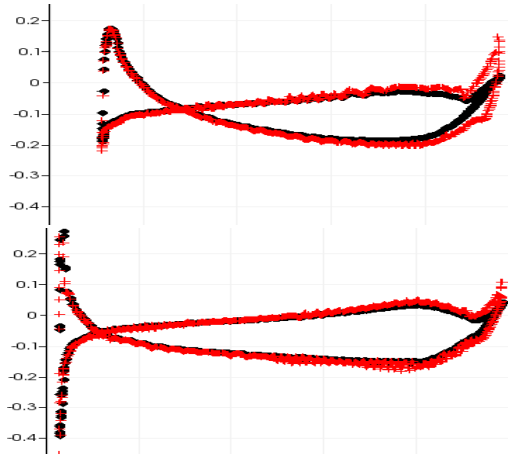
Fig. 5: CPP 1304: Surface pressure results (Cp) at two sections (upper: close to hub; lower: mid of blade) for viscid (*) and in-viscid (*) treatment of blade
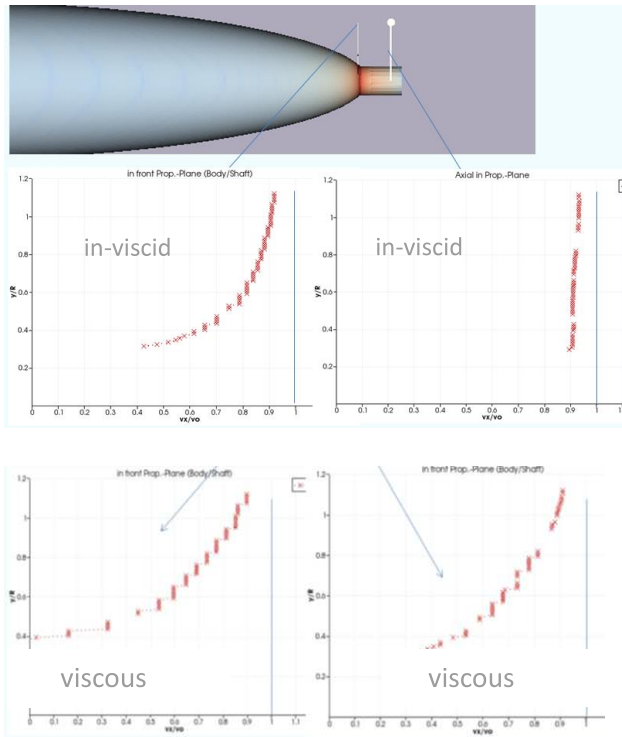

Fig. 6: Axial velocity profiles due to in-viscid and viscous BoR, ahead of (left) and at propeller (right)
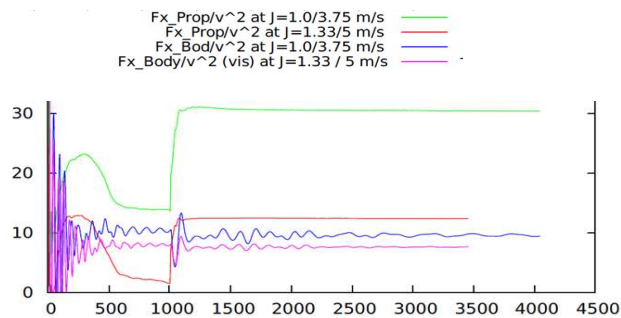

Fig. 7: History of forces on propeller 1304 and body of revolution for 2 propeller load conditions
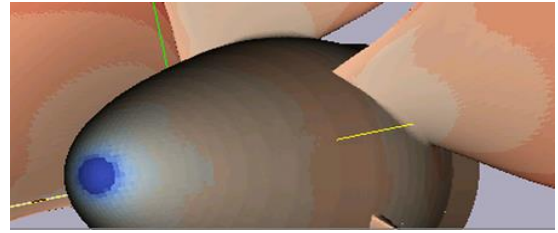

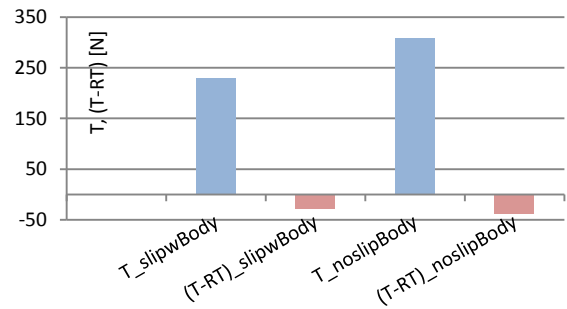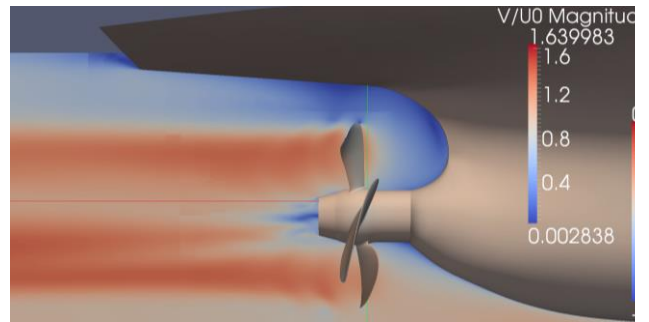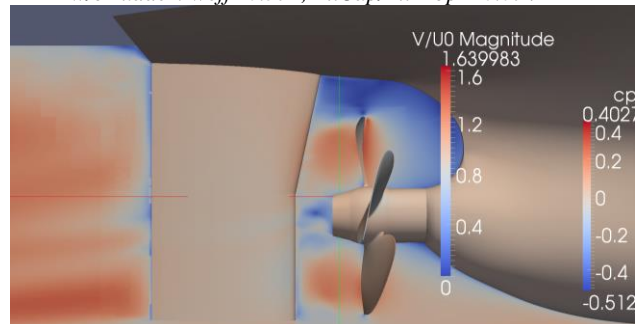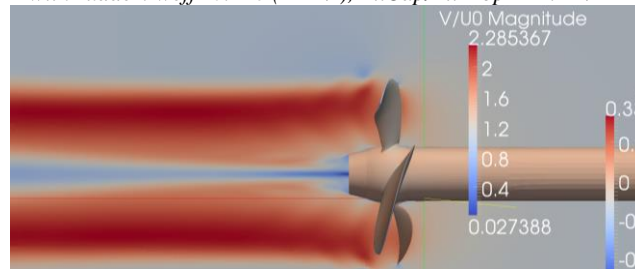Fig. 8: Low pressure region (blue) on hub cap of propeller 1304 when working behind the BoR

Fig. 9: Thrust and thrust deduction for propulsion of viscid and in-viscid body.

w/o rudder: weff=0.372, FxCap/FxProp=-0.07%

with rudder: weff=0.416 (+12%), FxCap/FxProp=+1.24%

POW J=0.45, weff=0.0, FxCap/FxProp=-0.82%

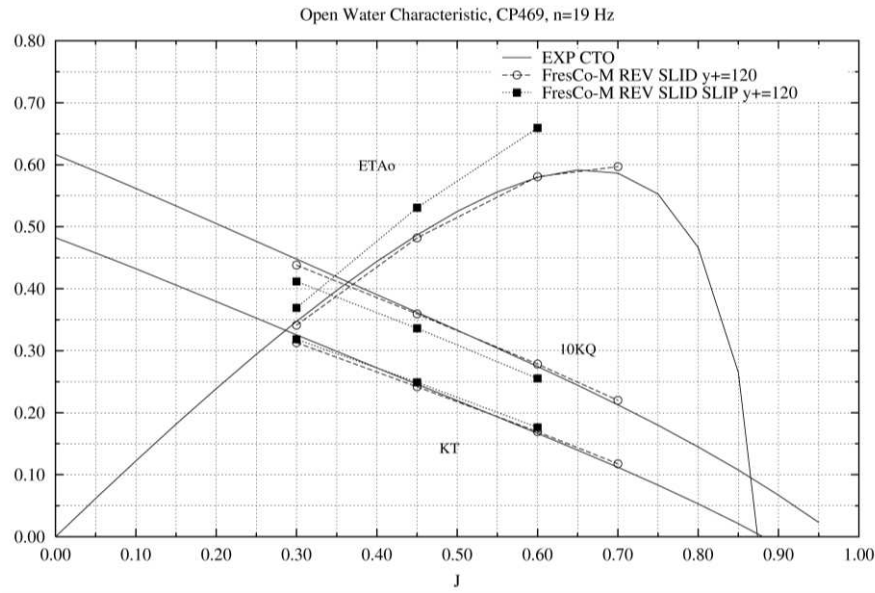Fig. 10: Velocity distribution V/U0 on mid ship of 'Nawigator' Vs=11 kts and for POW

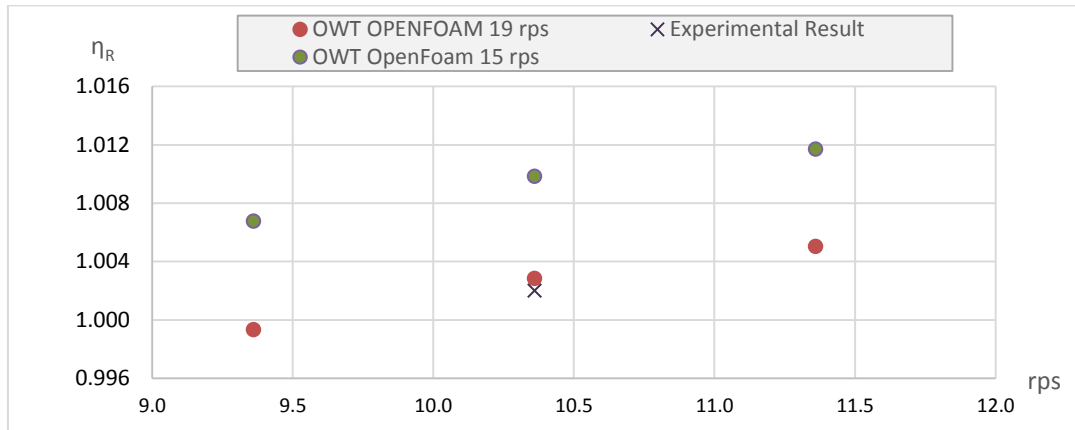Fig. 11: POW characteristics, EFD, CFD by HSVA comparing no-slip-wall and slip-wall on blades

Fig. 12: Development of η_R of CP 469 according to MMG, comparing in behind torque with open water torque calculated at different Reynolds-numbers
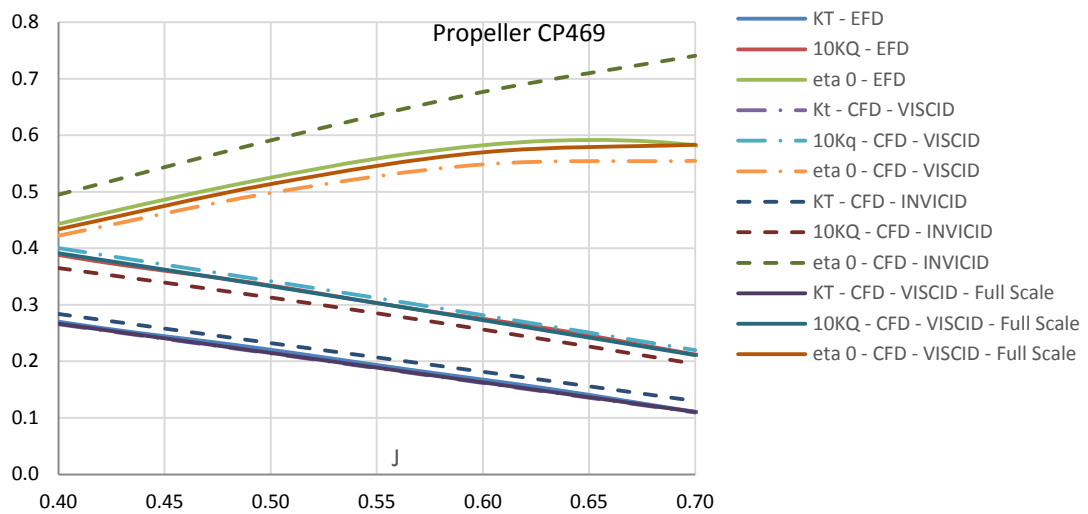

Fig. 13: POW characteristics, EFD, CFD by MILPER comparing no-slip-wall (at two scales) and slip-wall